

Calculation of the elastic scattering properties in a ultra-cold Fermi-Bose and Bose-Bose Rb-K vapor

M. Kemal Öztürk^{1,*} and Süleyman Özçelik^{1,†}

¹Physics Department, University of Gazi, 06500 Teknikokullar, Ankara, Turkiye

(Dated: Today)

The calculation of the elastic scattering properties of mixtures composed by rubidium and potassium atoms is reported and compared with experimental results in detail. The improved potentials for both molecular states the singlet $x^1\Sigma_g^+$ and the triplet $a^3\Sigma_u^+$ of the RbK are presented, and the scattering lengths a_t and the effective range r_e are calculated with the help of this potential using WKB and Numerov methods for Rb-K in the triplet and singlet state. In addition, the convergence of these scattering properties as the depending on a K_0 parameter is investigated using Quantum Defect Theory. The evaporative cooling other results that include the cross section and the spin-charge cross section, the rate coefficient as a function of the energy and the ultra-low temperature are also presented in this study.

PACS numbers: 32.80.Cy,32.80.Pj,34.20.Cf,34.50.Pi.

I. INTRODUCTION

Collisions of atoms at ultracold temperatures have received considerable attention because of their importance in the cooling and trapping of atoms [1] and molecules [2] and Bose Einstein condensation by Sympathetic cooling [3]. Ultracold mixtures of alkali metal atoms have recently been the subject of intensive experimental research, therefore the interest in the detailed knowledge of ultracold mixtures of alkali atoms has theoretically increased [4, 5]. Even, while collisions either between alkali often same species or between different isotopes have often been well characterized [6], collision between different alkali species have a still intensive exploring field. The condensed atoms and molecules may form a two-species Bose-Einstein condensate in which a new class of coherent phenomena is predicted to occur [7].

In an ultracold mixture, the interaction between the components is described in terms of a very important parameter, the interspecies s-wave scattering length. The character of the interaction between different alkali species in low-temperatures is determined by signs (\pm) and magnitude of the scattering length a : for bosonic atom with $a>0$ Bose condensate is stable, for $a<0$ it is unstable [8]. This parameter also determines the efficiency of the sympathetic cooling procedure [3]. In addition, knowledge of the scattering length is important in order to predict macroscopic properties of these mixed systems, such as the stability and phase separation of binary degenerate systems, or microscopic properties, such as the occurrence of resonances and the cross section and the spin-charge cross section in the interspecies collisions.

Accurate calculations of s-wave scattering length and effective range for diatomic potentials are important due

to the elastic collisions in these temperatures dominated s-wave scattering. In recent years, these quantities have been calculated by several theoretical methods [9, 10, 11, 12, 13]. The accurate determination of scattering length depends on choosing the interaction potentials. Collision processes at near-zero temperatures ($\sim \mu\text{K}$) are sensitive to the details of the interaction potentials between the colliding systems.

Previous theoretical and experimental calculations of the scattering length for Rb+K interaction have appeared in the literatures [3, 14]. The purpose of this paper, we are to calculate scattering lengths, effective ranges and phase shifts-cross section for the collisions of Rb+K at ultra-cold temperatures with the Semiclassical method (WKB) [15] and also solve the Schrödinger equation using Numerov method numerically [16]. We have investigated the convergence of some scattering properties obtained with help of these methods as the dependence of a K^0 parameter using Quantum Defect Theory [13]. The interaction of rubidium-potassium atoms in states ($^1\Sigma_g^+$) and ($^3\Sigma_u^+$) is described by short and long range potentials which includes the cutoff functions introduced to truncate the unphysical short-range contribution of the polarization potential near the origin [17]. Cutoff functions depending on the cutoff radius are adjusted by comparing the expressed potential form to the curve calculated with *ab-initio* by Rousseau et.al. [18]. Some results we have found are compared with theoretical values in the ref. [14] and the experimental result [3].

This paper is designed as the follow form, we discuss the computational process in Sec. 2. The interaction potentials, which play a crucial role in evaporate cooling and also determine many properties of the condensate, are given in Sec. 3. The ultracold scattering properties (the scattering length, effective range, phase shifts and the rate coefficients) are computed for collisions of the Rb-K isotope systems in the singlet and triplet states at ultra-cold temperatures in Sec. 4 and 5, respectively,

*Electronic address: ozturkm@gazi.edu.tr

†Electronic address: suleyman@gazi.edu.tr

and the convergences of the scattering range and the effective range are also investigated in detail. We conclude with brief conclusions.

II. PROCESSES

The scattering length is defined from the asymptotic behavior of the solution of the radial Schrödinger equation at zero energy:

$$\left[\frac{d^2}{dr^2} - 2\mu V(r)^{2S_{AB}+1} + k^2 + \frac{l(l+1)}{r^2} \right] y_l(r) = 0, \quad (1)$$

in atomic unit. Here μ is the reduced mass of the atomic system and $V(r)^{2S_{AB}+1}$ is the molecular potential between two atoms. Asymptotic behavior of the wave function is

$$y(r) = s r + s_0 \quad (2)$$

as $r \rightarrow \infty$, where s and s_0 are constants. The scattering length is given by

$$a = -\frac{s}{s_0}, \quad (3)$$

these constants are obtained by G. F. Gribakin using et al. using WKB method from semiclassical behavior and with help of the exact solution at zero-energy [19]. Eq. (3) is transformed to the form

$$a = \bar{a} \{1 - \tan\{\varphi - \pi/8\}\} \quad (4)$$

where \bar{a} is the “mean” or “typical” scattering length determined by the asymptotic behavior of the potential through the parameter $\gamma = \sqrt{2\mu\kappa}$ (μ is reduced mass, and $\kappa = c_6$ is Van der Waals constant) for atom-atom interactions:

$$\bar{a} = \frac{\Gamma(3/4)}{\Gamma(1/4)} \sqrt{2\gamma} \quad (5)$$

Scattering length also depends a semiclassical phase φ calculated at zero energy from classical turning point r_0 where $y(r_0) = 0$, to infinity,

$$\varphi = \int_{r_0}^{\infty} \sqrt{-2\mu V(r)^{2S_{AB}+1}} dr. \quad (6)$$

The total number of vibrational levels with zero orbital angular momentum was derived from φ , $N_{bd} = \{\varphi/\pi - (n-1)/2(n-2)\} + 1$, where n is are given by integer

value 6 for interaction of mixing or same species atoms [19]. A similar calculation of the semiclassical phase at negative energies, $E = -1/(2\mu a^2)$ yields $\varphi(E) = \varphi - \sqrt{\pi}\gamma^{2/n} a^{-(n-2)/n} \Gamma(\frac{1}{2}+1/n)/[(n-2)\Gamma(1+1/n)]$. It is often used for studying quantization of vibrational levels near the dissociation limit in diatomic molecules[20].

The effective range r_e can be written in terms of zero-energy solutions of the partial-wave equation if $y_0(r)$ is the solution of the partial-wave equation at $k = 0$ for zero-potential, and normalized as

$$y_0 = \frac{\sin(kr + \delta_0)}{\sin \delta_0} \quad (7)$$

as $k \rightarrow 0$, and if $y_0(r)$ is the normalized solution of the radial equation (1) for the s-partial wave at zero energy (for non-zero potential) as $y(r) \sim y_0(r)$ at $r \rightarrow \infty$. Then, effective range can be written as [15, 21]

$$r_e = 2 \int_0^{\infty} \{y_0^2(r) - y^2(r)\} dr. \quad (8)$$

This integral converges provided $y(r)$ approaches $y_0(r)$ rapidly enough as $r \rightarrow \infty$. This requires $V(r)$ to decrease faster than r^{-5} . For $-c_6/r^n$ potential type, this expression is adjusted by Flambaum et al.[22] using WKB method and the exact solution of the radial equation at zero-energy as

$$r_e = \frac{\sqrt{2\gamma}}{3} \left[\frac{\Gamma(1/4)}{\Gamma(3/4)} - 2\frac{\sqrt{2\gamma}}{a} + \frac{\Gamma(3/4)}{\Gamma(1/4)} \frac{4\gamma}{a^2} \right]. \quad (9)$$

The mean effective range may be easily obtained by replacing eq.(4) into eq. (9) as

$$\bar{r}_e = \frac{\sqrt{\gamma}}{3} \left[\frac{\frac{\sqrt{2}\Gamma(1/4)}{\Gamma(3/4)} - \frac{4\sqrt{\gamma}}{\bar{a}(1+\tan(\frac{1}{8}(\pi-8\varphi)))}}{\frac{\Gamma(3/4)}{\Gamma(1/4)(1+\tan(\frac{1}{8}(\pi-8\varphi)))^2} \frac{4\sqrt{2\gamma}}{\bar{a}^2}} \right]. \quad (10)$$

The low-energy scattering is dominated by the contribution $l = 0$. At values of k close to zero, the $l = 0$ phase shifts δ_0 can be represented by a power series expansion in k [23]

$$k \cot \delta_0 = -\frac{1}{a} + \frac{1}{2} r_e k^2 + o(k^3). \quad (11)$$

This expression is known as Bethe formula.

III. INTERACTION POTENTIALS

The interaction between the atoms has two features: First, the potential at large distances behave as an inverse power of the interatomic distance, $V(r) = -\kappa/r^n$

with $n = 6$ for spherically symmetric two atoms in their ground state. The asymptotic parameter $\kappa \equiv c_6$ is known quite well for most atomic pairs of interest. Second, for atoms other than hydrogen and helium the potential curve is usually quite deep and also the electron-exchange part of the atomic interaction is repulsive at smaller distance as for the singlet and triplet terms of alkali-metal atoms. “Deep” here means that the wave functions of the atomic pair oscillate many times within the potential well, even at very low collision energies. The interatomic potential supports a large number of vibration levels. This latter feature enables one to use the semiclassical approximation to describe the motion of atoms within potential well [22].

The mixing alkali-metal atoms have unpaired electron spin $s = 1/2$ in the ground state. Therefore, the interaction between two different alkali atoms in the ground state results in the formation of a diatomic molecule, which is described by two terms corresponding to the total spin $s_{ab} = s_a + s_b$ of the system equals to 1 or 0. The state with $s_{ab} = 0$ and 1 corresponds to the singlet state and triplet state, respectively. The probability of the spin exchange is determined by both the dependence of potential curves on the internuclear distance r and the splitting between singlet and triplet terms. The exchange interaction is analytically calculated using the surface integral method by Smirnov and Chibisov [24], which yields

$$v_{exc.}(r) = \frac{1}{2}(v_u - v_g) = r^\alpha e^{(-\beta r)} J. \quad (12)$$

Where α, β and C are constants. In this equation, J is given by $\sum_n f_n J_n r^n$, here, f_n are fit constants adjusted by fit program for the best R square in this paper, and J_n are the integral constants. For Rb-K, these values of constants taken from the paper of Smirnov and Chibisov are given in Table I. The long-range part of the interaction potential is given by

$$v_{long-range} = -\sum_m^{even} \frac{C_m}{r^m} f_c(r), \quad (13)$$

this term is the sum of Van der Waals terms, multiplied by the relevant cutoff function $f_c(r)$ to cancel $1/r^n$ divergence at small distances. The area under r axis of the interaction potential is very important to specify the ultracold scattering properties, and its value is calculated from the eq. (6). For any different two potential, when it has same semiclassical phase shifts, the scattering properties aren't affected from the change of other parameters of potential such as the depth of potential [25]. It is the fact that theoretical potential should actually adopt with *ab-initio* one. Therefore, in the singlet state, the some sensitive Wan der Waals parameters taken from ref. [26] was multiplied with fit parameter C_f^c . As shown in the Fig.1, it concludes that the potentials are excellent adapt due to R square, and we may also name the C_f^c as the corrected constant for Wan der Waals parameters in singlet

and triplet state, and this technique may be useful for other studies. C_6 , C_8 and C_{10} parameters were taken from A. Derevianko et al.'s paper (Ref. [26]). The cutoff function is analogous to that used for the H-H $^3\Sigma_u^+$ potential [27].

$$f_c(r) = \xi(r - r_c) + \xi(r_c - r)e^{-(\frac{r_c}{r}-1)^2}, \quad (14)$$

Where $\xi(z)$ is unit step function $\xi(z) = 1(0)$, when $r > (<)0$. There, the only free parameter for the potential sum is the cutoff radius r_c , governing the decrease of the function $f_c(r)$ for $r < r_c$. The potential of the collisions Rb+K consists of above the expressed two terms, the sum of Eqs. (12) and (13), is given as

$$V^{2s_{AB}+1}(r) = V(r)_{long-range} + (-1)^{s_{ab}} V(r)_{exc.} \quad (15)$$

The magnitude of the cutoff parameters r_c has been adjusted by comparing this potential with the experimental curve in triplet state obtained by Rousseau et.al. [18] using *ab-initio* for the large range.

The most relevant potential curves for different r_c values are represented in Fig.1, together with the experimental calculation and their R square values (inset). Owing to R square value, there is in excellent agreement between experimental and theoretical curves for the cutoff radius determined from the fit curve.

IV. THE CONVERGENCE AND CALCULATION SCATTERING LENGTH AND EFFECTIVE RANGE OF Rb + K

In this section, the scattering length and the effective range for the collisions of Rb+K in singlet and triplet state at ultra-cold temperature have been calculated with semiclassical method (WKB) [15] and also determined by solving the Schrödinger equation by Numerov method [16] for the potential given with Eq.(15). Also, we investigated the convergence of these scattering properties as a function of energy parameter (K^0) using Quantum Defect Theory[13].

In third column of Table II, the results of the scattering length calculated from Eq.(4) with help of the WKB method are represented for the collision of mixtures composed by rubidium and potassium atoms in singlet and triplet state described with the potentials in eq.(15) characterized by the term of cutoff radius. Some parameters are important in the determination of $a(a.u.)$ for WKB method. We also obtain these parameters, the mean scattering length \bar{a} and the zero-energy semiclassical phases φ , given in Table III using values of asymptotic parameter γ . Here, the mean scattering length with asymptotic behavior of the potential in eq.(15) has been calculated from equation (5).

For calculation numerically scattering length, we obtained s-wave phase shift δ_0 using the potentials in

eq.(15), then we do it by solving radial equation using Numerov algorithm at $e = k^2/2\mu$ in atomic unit and finding δ_0 from the asymptotic behavior of the wave function $y(r) = \sin(kr + \delta_0)$. The phases at small momenta k are used to extract the scattering length numerically from $a = -\lim_{k \rightarrow 0} (d\delta_0/dk)$. The scattering lengths obtained via this method are given in the fourth columns of Table II. The results obtained in two methods are compared with values found in the literature .

From the measured thermalization rate, using the model presented in Ref.[28], the large value for the zero-energy s-wave scattering length are obtained using conventional double magneto-optical trap (MOT) apparatus [29, 30]. G. Modugno, G Ferrari and et. al have estimated a direct measurement of the scattering lengths for the ^{41}K - ^{87}Rb pair [3]. They also deduced the collisional behavior of other isotope combinations by the help of mass scaling in the experimental columns of Table II. [14]. Then, for the ^{40}K - ^{87}Rb and ^{41}K - ^{87}Rb pairs, Simoni et al. investigated the scattering properties in the presence of several magnetic field [31].

As shown in the Table II, the scattering lengths calculated for the collisions of rubidium- potassium pairs is in excellent agreement with the experimental scattering length when $V(r)$ potential has the excellent adopt with *ab initio* curve due to the best R square value.

Even our results shows that the stability of large condensates requires repulsive interactions (positive a), whereas for attractive interactions (negative a) it is unstable, only a finite number of atoms can be found in condensate state in a trap. As shown Table II, the scattering lengths found as negative value due to changes in the $V(r)$, lead to a condensate triplet state where the number of atoms is limited to a small critical value determined by the magnitude of a . In contrast, we have observed the positive scattering lengths that produce stable condensates. Also, from the scattering length given as a function of the semiclassical phase shift in the eq. (4), we say that the minor changes in phase shifts have strongly affected the scattering amplitude. It concludes that the ultra-cold scattering depends on the potential changes given by phase. It must be remarked that our emphasis for ^{41}K - ^{87}Rb pair is weakly dependent on the number N_{bd} of bound states supported by *ab-initio* potential. The numbers of bound states N_{bd} have been computed in the intervals 108-110 and 32-33 for both singlet and triplet states, respectively. The numbers of bound states of the singlet state is consistent with the result ($N_b = 32$) obtained ref.[14] In addition, the mass scalling from one isotope to the others depends more strongly on n_s . The calculations in this paper shows that due to being boson-fermion, of great interest also is the ^{40}K - ^{87}Rb pair, for which we find a negative and probably large interspecies scattering length agreed with other result in Table II which implies an efficient sympathetic cooling of the fermionic species down to the degenerate regime [14].

Effective ranges calculated using Numerov and WKB methods in the function of phase for the triplet rubidium-

Potassium potentials are presented in Table IV together the calculation of semiclassical phase shifts. The close agreement between the calculations of r_e from Eqs.(8) and (11) confirms the accuracy of the numerical integration of the partial-wave equation. The size of the scattering lengths and effective ranges is closely related to the position of the last vibration bound states of the energy curves, as can be anticipation by inspection of Eq.(3) and number of vibrational levels $n_s(\varphi/\pi)$ which, consistent with Levinson's theorem, show that as the binding energy of the highest level tends to zero, the scattering length tends to \pm infinity [15].

Analytical calculations of scattering lengths are important in investigation of convergence of the scattering length and the effective range. In many approaches used to solve collision problems in atomic physics, the tree dimensional configuration space is divided into two regions separated by a spherical shell (a core boundary) of radius ρ . In the inner region ($r < \rho$) the short-range interaction between two colliding particles is very complicated and a scattering equation must be solved independently for each combination of particles. In contrast, if ρ is chosen sufficiently large the scattering problems in the outer region ($r > \rho$) may be reduced to potential scattering with the long-range potential accurately approximated by simple analytical expression. A numerical solution in this region is usually easily approachable [32]. One of these methods is Quantum Defect Theory described by Gao [13].

Quantum defect theory of atomic collisions is presented by Bo Gao. Based on the exact solutions of the Schrödinger equation for an attractive $1/r^6$ potential, the theory provides a systematic interpretation of molecular bound states and atom-atom scattering properties and establishes the relationship between them. Bo gao finds a definition for the scattering length and the effective range and s-wave at zero energy as

$$\left. \begin{aligned} a_{l=0} &= \frac{2\pi}{[\Gamma(1/4)]^2} \frac{K^{0-1}}{K^0} \beta_6 \\ r_{l=0} &= \frac{[\Gamma(1/4)]^2}{3\pi} \frac{[K^0]^2 + 1}{[K^0]^2} \beta_6 \end{aligned} \right\} \quad (16)$$

where $\beta_6 = (2\mu C_6)^{1/4}$ and K^0 is the analytic function of energy.

Figure 2 show the scattering length and the effective range curve plotted with the help of eqs. (16) and values(dotted points) obtained by the mean WKB formulas, eqs.(5) and (10).

Our graphical representations show that as K^0 goes infinity, the QDT results converges excellently to values obtained by WKB method in Fig. 2 . Even, it may be said that the different calculating of the scattering properties in these two method gives similar results for any ultracold atom-atom collision (e.g. ref. [33]).

V. PHASE SHIFTS AND CROSS SECTION

Scattering length describes behavior of the atom scattering at low energy, and phase shifts are important parameter for it. Furthermore, at a low energy, E , of relative motion the phase-shift is $N_{bd}\pi + \delta$, where N_{bd} is the number of bound states. The phase shift can be calculated by fitting the solution $y(r)$ to $\sin(kr)$ and $\cos(kr)$, the asymptotic solutions of Eq. (1). Let S_i and C_i denote $\sin(kr_i)$ and $\cos(kr_i)$, respectively. Fitting at r_i and r_j we find, for a small shift [15, 16],

$$\delta \approx \tan(\delta) = -\frac{S_i y_j - S_j y_i}{C_i y_j - C_j y_i}, \quad (17)$$

where $r_{i,j} = r_0 + (i, j)h$ (h is the step-length). we show the numerical phase shifts (module π) in Fig. 3 it is also known in more tex book that the low energy scattering is always dominated by the $l = 0$ partial wave the corresponding phase shift being given by

$$\delta_0 = -ka \quad (18)$$

which is shown for all Rb+K collisions in Fig. 3. Here, to plot phase shifts we used the semiclassical scattering lengths. As momenta goes zero, for $l = 0$, the s-phase shifts are very close in the singlet state. it concludes that when a gas mixture composed of fermion-boson or boson-boson is cooled below a critical temperature, the mixing atoms condensates in the lowest quantum state. Moreover, if the atoms are bosons, a cloud of atoms occupies the same quantum state at low temperature. If the atoms are fermions, cooling gradually brings the gas closer to being a ‘Fermi sea’ in which exactly one atom occupies each low-energy state [34].

As shown in fig. 3, their scattering lengths are unstable against collapse except the ^{40}K - ^{85}Rb . For these mixtures of composed by fermion-boson, the condensates are more attractive than that of boson-boson as reported in Table III. In this case, the fermionic cloud cannot shrink below a certain size determined by the Pauli Exclusion Principle due to bosonic cloudy [34].

Elastic singlet and triplet cross sections between two atoms, can be defined by

$$\sigma_{el.}^{S,T} = \frac{4\pi}{k^2} \sum_{l=0}^{\infty} (2l+1) \sin^2 \delta_l^{S,T}, \quad (19)$$

where S and T stand for singlet and triplet, respectively. We have obtained the phase shifts (δ_l) and cross sections ($d\sigma_l$) for the collision $^{85}\text{Rb}+^{40}\text{K}$ with $l = 2, 4$ values of the angular momentum and different energies using Numerov method. They are listed in Table IV. this table shows that the δ_l and $d\sigma_l$ for very low energy have large values lead to the being of more collisions. In the ultracold gas of the mixing alkali metal atoms dominated by

the $l = 0$ contribution, the cross sections are given by $\sigma_{el.}^{S,T} = 8\pi a_{S,T}^2$ and $\sigma_{el.}^{S,T} = 4\pi a_{S,T}^2$ for boson-boson systems and boson-fermion systems, respectively [35]. The spin-change cross sections are calculated from the singlet and triplet phase shifts by

$$\sigma_{sc} = \frac{\pi}{k^2} \sum_{l=0}^{\infty} (2l+1) \sin^2(\delta_l^T - \delta_l^S). \quad (20)$$

In the limit of low energies, Eq. 20 is transformed to $\sigma_{sc.} = \pi(a_T^2 - a_S^2)$ [10]. In addition, this parameter is known as spin-flip collisions lead to trap losses [36]. The zero-energy cross sections for the selected mixing atoms are $3.29010^{+11}a_0^2(=9.21310^{-10}\text{m}^2)$ and $3.06510^{10}a_0^2(=8.58410^{-11}\text{m}^2)$ for singlet and triplet states of the ^{40}K - ^{85}Rb , and $4.700 \cdot 10^{+11}a_0^2(=1.316 \cdot 10^{-09}\text{m}^2)$ and $8.152 \cdot 10^{+10}(=2.28310^{-10}\text{m}^2)$ for singlet and triplet states of the ^{39}K - ^{87}Rb , respectively. Spin-charge cross sections are also $7.45910^{+10}a_0^2(=2.08710^{-10}\text{m}^2)$ in the ^{40}K - ^{85}Rb and $2.27610^{+10}a_0^2(=6.37310^{-11}\text{m}^2)$ in the ^{39}K - ^{87}Rb .

We assume the velocity distribution is Maxwellian characterized by a kinetic temperature T , and we define mean elastic and spin-change cross sections by

$$\bar{\sigma}(T) = \frac{1}{(k_B T)^2} \int_0^{\infty} \sigma(E) E e^{(-E/k_B T)} dE. \quad (21)$$

Assuming equal temperatures of the each pair of isotopes in the Rb-K vapor, the corresponding rate coefficients are given by

$$\mathfrak{R}^{S,T,SC} = \left[\frac{8k_B T}{\pi\mu} \right] \bar{\sigma}(T). \quad (22)$$

We show values of the cross sections as depending on the energy in the (m^2) in Fig. 4 for E up to 10^{-2} (a.u.) and list values of the spin-change $2s_{AB} + 1$ in cm^3s^{-1} in the Table VI for T up to 1K.

Figure 4 gives cross sections for some interaction of atoms. They show that in the low energies, less partial-wave contributes to scattering. As shown in figure fermion-boson $^{85,87}\text{Rb}+^{40}\text{K}$ collisions display different properties. it may be said that $^{85}\text{Rb}+^{40}\text{K}$ is more stability than $^{87}\text{Rb}+^{40}\text{K}$, because later has less partial waves with decreasing values of the energy for both singlet and triplet state and its total cross sections are in very low values in the same higher energy region.

VI. CONCLUSIONS

The elastic scattering properties for the collision of the two mixing atoms in a limited range of moment ($k < \bar{a}^{-1} \approx 0.01\text{a.u.}$ for Rubidium-Potassium isotopes) at

low temperatures are sensitive to the details of interaction potentials. Scattering properties such as the scattering length, the effective range, the phase shift and the cross section have been computed using semiclassical and a numeric methods for the $V(r)$ potentials as dependence of cutoff radius adjusted by comparing with the experimental potential for ultra-cold rubidium-potassium isotopes collision. We investigated the convergence of these scattering properties as the depending of core radius and

K^0 parameter using Quantum Defect Theory. Cross section was obtained as $\sim 1.010^{-10}m^2$ at low energy. The phase shifts, an intermission parameter for scattering length and effective range, has linear manner at small momenta $k < \bar{a}^{-1}$. So, it has been determined by computing numerically and analytically for $V(r)$ potential. In bigger momenta than the inverse mean scattering length, the phase shifts display parallel behavior as the dependence of semiclassical phase shift, $\delta_0(k) \sim \varphi - ka$.

-
- [1] F. Dalfovo et al., 1999 Rev. Mod. Phys. 71 463.
 [2] E Bodo et al., 2002 J. Phys. B:At. Mol Opt. Phys. 35 1.
 [3] G. Mudugno, G. Ferrari, et al., 2001 Science 264 1320.
 [4] V. Venturi et al., 2001 J. Phys. B:At. Mol Opt. Phys. 34 4339.
 [5] Z. Hadzibabic, C. A. Stan et al., 2002 Phys. Rev. Lett. 88 160401.
 [6] J. Weiner et al., Rev. Mod. Phys. 71, 1(1999).
 [7] E. Timmermans, P. Tommasini et al., 1999 Phys. Rev. Lett. 83 2691.
 [8] V.V. Flambaum, G. F. Gribakin, and C. Harabati 1999 Phys. Rev. A 59 1998.
 [9] N. Balakrishnan, R. C. Forrey, and A. Dalgarno 1998 Phys. Rev. Lett. 80 3224.
 [10] R. Côté, A. Dalgarno, and M. J. Jamieson 1994 Phys. Rev. A 50 399.
 [11] M. Marinescu 1994 Phys. Rev. A 50 3177.
 [12] Zbigniew Idziaszek et al.1999 J. Phys. B:At. Mol Opt. Phys. 32 L205.
 [13] Bo Gao 1998 Phys. Rev. A 58 4222.
 [14] G. Ferrari, M. Inguscio, et al., 2002 Phys. Rev. Lett. 89 053202.
 [15] Charles J. Joachain 1975 Quantum Collision Theory (North-Holland, Amsterdam).
 [16] R. Côté, M. J. Jamieson 1995 Journal of Computational Physics 118 388.
 [17] M. Marinescu, H.R. Sadeghpour, and A. Dalgarno 1994 Phys. Rev. A 49 982.
 [18] S. Rousseau, A. R. Allouche, and M. Aubert-Fre'con, 2000 J. Molec. Spectroscopy 203 235.
 [19] G. F. Gribakin and V. V. Flambaum 1993 Phys. Rev. A 48, 546.
 [20] R. J. LeRoy and R. B. Bernstein, 1970 J. Chem. Phys. 52, 3869; J. Trost, C. Eltschka, and H. Friedrich, 1998 J. Phys. B 31, 361.
 [21] E. G. M. van Kempen et al., 2002 Phys. Rev. Lett. 88 93201.
 [22] V.V. Flambaum, G. F. Gribakin, and C. Harabati 1999 Phys. Rev. A 59 1998.
 [23] H. A. Bethe 1949 Phys. Rev. A 26 38.
 [24] B.M. Smirnov and M. I. Chibisov 1965 Soviet Physics JETP 21 624.
 [25] M. Kemal Öztürk and S. Özçelik, Acta Plonica Physica (submitted).
 [26] A. Derevianko et al., 1999 Phys. Rev.Lett. 82 3589.
 [27] D. G. Friend and R. D. Eppers 1980 J. Low Temp. Phys. 39 409.
 [28] A. Mosk et al., 2001 Appl. Phys. B 73 791.
 [29] L. G. Marcassa et al., 2000 Phys. Rev. A 63, 013413 .
 [30] J. Goldwin et al., 2002 Phys. Rev. A 65, 021402(R).
 [31] A. Simoni et al. 2003 Phys. Rev. Lett. 90 163202.
 [32] Radoslaw Szymkowski, J. Phys A: Math. Gen. 1995 (28) 7333.
 [33] M. Kemal Öztürk and S. Özçelik, (unpublished).
 [34] James R. Anglin and Wolfgang Kertterle 2002 Nature 416 211.
 [35] W. Geist, L. You and T. A. B Kennedy 1999 Phys. Rev. A 59, 1500.
 [36] A. Derevianko et al., 2001 Phys. Rev. A 64 011404.

TABLE I: Potential coefficients for Rb-K atoms in singlet and triplet state.

	$^1\Sigma_g^+$	$^3\Sigma_u^+$
$10^{-3}f_1$	345	-345
$10^{-3}f_2$	1.0	-1.0
$10^{-3}f_3$	1.0	-1.0
$10^{-3}J_1^1$	5.0	5.0
$10^{-4}J_2^1$	4.0	4.0
$10^{-3}J_3^1$	7.0	7.0
α^1	5.256	5.256
β^1	1.119	1.119
$10^{-4}C_6^{2,3}$	1.502	4.274
$10^{-5}C_8^{2,4}$	5.922	5.922
$10^{-7}C_{10}^2$	6.726	6.726

¹ Ref.[24], ²Ref.[26].

³The fit constant defined in the text is $C_6^S = 3.514$

⁴The fit constant defined in the text is $C_8^{S,T} = 0.865$

TABLE II: Scattering lengths a (in atomic units) for ultracold rubidium-potassium mixtures in singlet and triplet states.

		^{39}K			^{40}K			^{41}K		
		a^i	a^{ii}	a^{iii}	a^i	a^{ii}	a^{iii}	a^i	a^{ii}	a^{iii}
^{85}Rb	S	136.73	136.76	-	161.84	161.807	-	212.56	212.55	-
	T	56.983	56.952	58_{-6}^{14}	-49.364	-49.390	-38_{-17}^{57}	271.568	306.016	329_{-55}^{1000}
^{87}Rb	S	-3.121	-3.197	-	23.927	23.926	-	54.459	54.456	-
	T	36.854	36.894	31_{-6}^{16}	-200.05	-200.04	-261_{-159}^{170}	167.29	167.28	163_{-12}^{57}

ⁱCalculated using semiclassical method for the $V(r)$ potential.

ⁱⁱCalculated using Numerov method for the $V(r)$ potential.

ⁱⁱⁱRef.[14], scattering lengths have been measured with help of the conventional cross-dimensional thermalization technique.

TABLE III: Mean scattering lengths a (in atomic units) and semiclassical phase shifts for ultracold rubidium-potassium mixtures in singlet and triplet states.

	^{39}K		^{40}K		^{41}K	
^{85}Rb a_s, φ	93.65	339.254	94.056	342.202	94.449	345.072
a_t, φ	68.393	101.089	68.690	101.967	68.977	102.823
^{87}Rb a_s, φ	93.82	340.486	94.230	343.467	94.627	346.369
a_t, φ	68.517	101.357	68.817	102.244	69.107	103.108

TABLE IV: Effective ranges r_e (in atomic units) for rubidium-potassium atom scattering.

	^{39}K		^{40}K		^{41}K	
	r_e^i	r_e^{ii}	r_e^i	r_e^{ii}	r_e^i	r_e^{ii}
^{85}Rb S	155.323	155.321	140.841	140.841	139.505	139.502
T	295.498	295.400	1534.41	1534.38	124.996	124.989
^{87}Rb S	511.371	511.387	6637.97	6635.634	983.868	983.527
T	838.647	838.413	386.47	386.535	103.87	102.995

ⁱCalculated using semiclassical method for $V(r)$.

ⁱⁱCalculated using Numerov method for $V(r)$.

TABLE V: Cross sections (in the m^2 unit) and phase shifts calculated for $V(r)$ potential using numerical Numerov method.

		$^x\text{Rb-}^y\text{K}$						
$\text{Lg}_{10}(\text{E})$	L	Factor	$^{85-39}$	$^{85-40}$	$^{85-41}$	$^{87-39}$	$^{87-40}$	$^{87-41}$
δ_0	-14.99	2 10^{-3}	5.17	4.93	5.86	3.28	4.48	2.69
		4 10^{-3}	5.50	5.57	6.61	3.64	5.36	3.36
	-11.57	2 -	0.256	0.245	0.289	0.165	0.223	0.136
		4 -	0.271	3.261	0.322	1.562	0.265	0.169
$d\sigma$	-14.99	2 10^{-12}	5.00	4.92	7.67	2.24	4.73	1.58
		4 10^{-12}	3.63	3.55	5.61	1.62	3.43	1.14
	-11.08	2 10^{-12}	4.57	4.52	6.63	2.15	4.33	1.53
		4 10^{-12}	3.32	3.26	4.85	1.56	3.14	1.12

TABLE VI: Singlet, Triplet and Spin-change rate coefficients for different isotops of the mixed Rb-K. The numbers in brackets denote multiplicative powers. a) $^{85}\text{Rb-}^{39}\text{K}$, b) $^{85}\text{Rb-}^{40}\text{K}$, c) $^{85}\text{Rb-}^{41}\text{K}$, d) $^{87}\text{Rb-}^{39}\text{K}$, e) $^{87}\text{Rb-}^{40}\text{K}$, f) $^{87}\text{Rb-}^{41}\text{K}$.

$\log_{10}(\text{K})(\text{a})$	$R_S(\text{m}^3\text{s}^{-1})$	$R_T(\text{m}^3\text{s}^{-1})$	$R_{SC}(\text{m}^3\text{s}^{-1})$	$\log_{10}(\text{K})(\text{d})$	$R_S(\text{m}^3\text{s}^{-1})$	$R_T(\text{m}^3\text{s}^{-1})$	$R_{SC}(\text{m}^3\text{s}^{-1})$
-8	2.00(-12)	5.48(-12)	1.30(-16)	-8	2.02(-12)	5.50(-12)	2.72(-16)
-7	1.13(-12)	3.09(-12)	7.34(-17)	-7	1.12(-12)	3.05(-12)	1.51(-16)
-6	6.77(-14)	1.80(-13)	1.41(-15)	-6	6.82(-14)	1.78(-13)	1.89(-15)
-5	4.75(-14)	8.57(-14)	1.45(-14)	-5	5.23(-14)	8.47(-14)	1.95(-14)
-4	5.33(-14)	9.27(-15)	5.17(-14)	-4	4.75(-14)	9.13(-15)	5.56(-14)
-3	1.56(-13)	4.19(-16)	1.74(-13)	-3	2.08(-14)	4.13(-16)	2.64(-14)
-2	3.71(-13)	1.59(-17)	4.31(-13)	-2	3.05(-14)	1.56(-17)	3.53(-14)
-1	5.45(-13)	1.44(-18)	6.36(-13)	-1	1.29(-13)	1.42(-18)	1.50(-13)
0	6.52(-13)	4.35(-19)	7.61(-13)	0	1.84(-13)	4.32(-19)	2.15(-13)
$\log_{10}(\text{K})(\text{b})$	$R_S(\text{m}^3\text{s}^{-1})$	$R_T(\text{m}^3\text{s}^{-1})$	$R_{SC}(\text{m}^3\text{s}^{-1})$	$\log_{10}(\text{K})(\text{e})$	$R_S(\text{m}^3\text{s}^{-1})$	$R_T(\text{m}^3\text{s}^{-1})$	$R_{SC}(\text{m}^3\text{s}^{-1})$
-8	2.01(-12)	5.53(-12)	4.39(-18)	-8	2.00(-12)	5.48(-12)	1.30(-16)
-7	1.09(-12)	2.99(-12)	2.37(-18)	-7	1.13(-12)	3.09(-12)	7.34(-17)
-6	6.40(-14)	1.75(-13)	1.83(-16)	-6	6.77(-14)	1.80(-13)	1.41(-15)
-5	3.28(-14)	8.33(-14)	2.22(-15)	-5	4.75(-14)	8.57(-14)	1.45(-14)
-4	1.97(-14)	8.92(-15)	1.63(-14)	-4	5.33(-14)	9.27(-15)	5.17(-14)
-3	2.47(-14)	4.03(-16)	2.83(-14)	-3	1.56(-13)	4.19(-16)	1.74(-13)
-2	1.16(-14)	1.52(-17)	1.34(-14)	-2	3.71(-13)	1.59(-17)	4.31(-13)
-1	7.75(-14)	1.39(-18)	9.06(-14)	-1	5.45(-13)	1.44(-18)	6.36(-13)
0	9.56(-14)	4.24(-19)	1.12(-13)	0	6.52(-13)	4.35(-19)	7.61(-13)
$\log_{10}(\text{K})(\text{c})$	$R_S(\text{m}^3\text{s}^{-1})$	$R_T(\text{m}^3\text{s}^{-1})$	$R_{SC}(\text{m}^3\text{s}^{-1})$	$\log_{10}(\text{K})(\text{f})$	$R_S(\text{m}^3\text{s}^{-1})$	$R_T(\text{m}^3\text{s}^{-1})$	$R_{SC}(\text{m}^3\text{s}^{-1})$
-8	2.03(-12)	5.58(-12)	1.31(-18)	-8	1.96(-12)	5.36(-12)	1.27(-16)
-7	1.05(-12)	2.88(-12)	6.76(-19)	-7	1.11(-12)	3.03(-12)	7.19(-17)
-6	6.23(-14)	1.72(-13)	4.89(-18)	-6	6.63(-14)	1.76(-13)	1.38(-15)
-5	2.94(-14)	8.10(-14)	6.08(-17)	-5	4.65(-14)	8.39(-14)	1.42(-14)
-4	3.98(-15)	8.59(-15)	8.95(-16)	-4	5.22(-14)	9.08(-15)	5.06(-14)
-3	1.14(-14)	3.88(-16)	1.20(-14)	-3	1.52(-13)	4.11(-16)	1.71(-13)
-2	4.53(-14)	1.45(-17)	5.21(-14)	-2	3.64(-13)	1.55(-17)	4.22(-13)
-1	2.49(-14)	1.36(-18)	2.91(-14)	-1	5.33(-13)	1.41(-18)	6.23(-13)
0	1.50(-14)	4.03(-19)	1.72(-14)	0	6.39(-13)	4.26(-19)	7.45(-13)

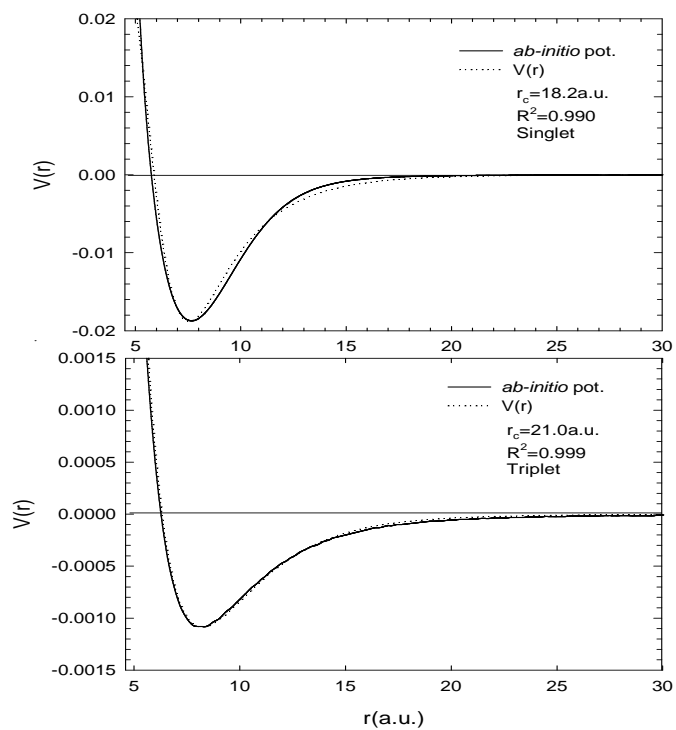


FIG. 1: Potential energy (dotted line) curves obtained as compared with experimental (solid line) potential curve for the best cutoff radii in the singlet and triplet states of the molecular KRb. The insets show R^2 values and cutoff radii

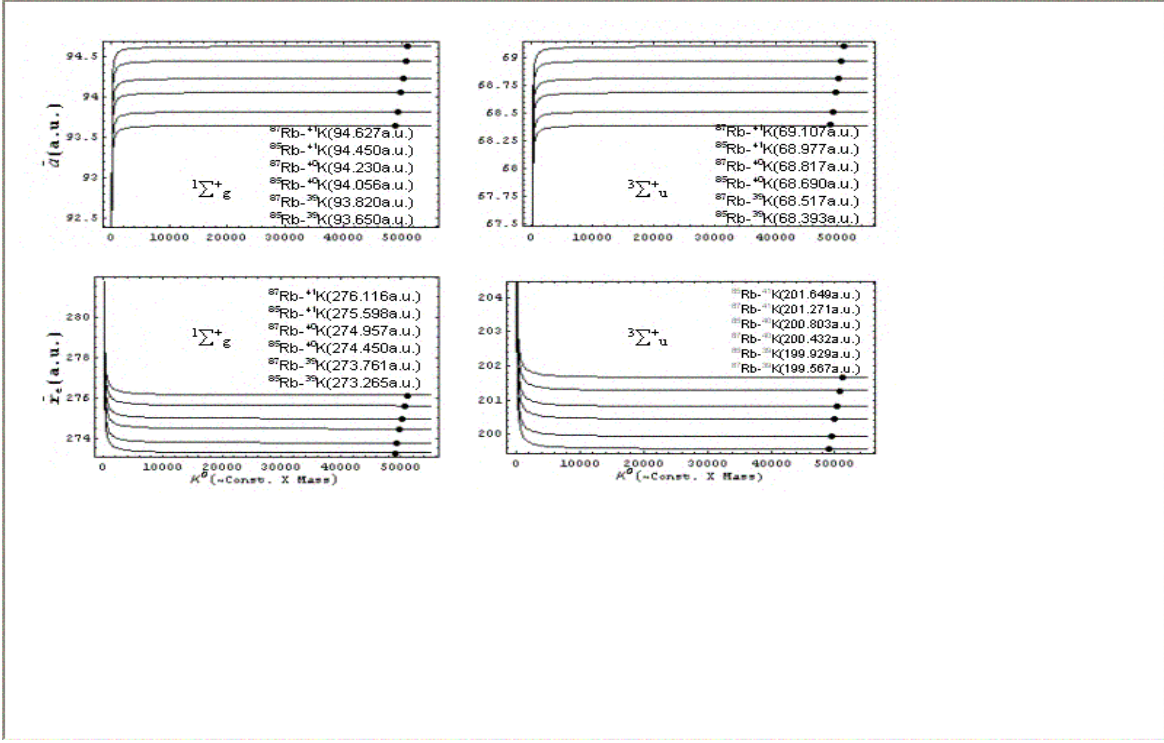


FIG. 2: Convergence of the scattering length and the effective range calculated with QDT as a function of K parameter when K goes infinity.

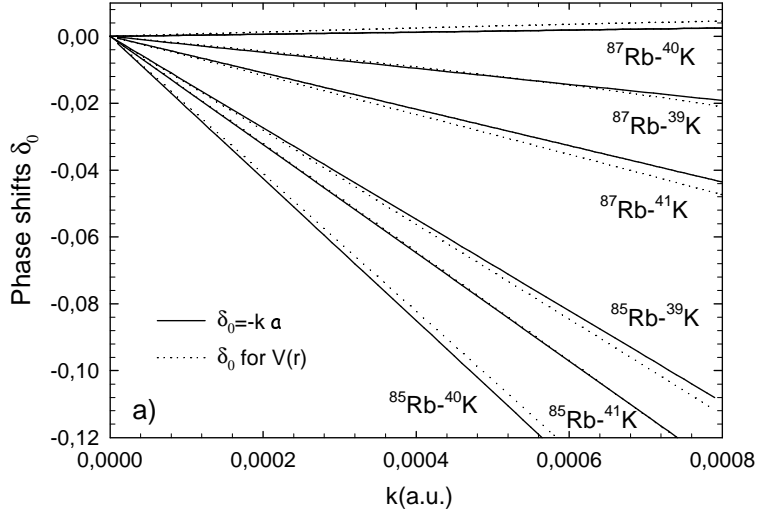


FIG. 3: s-wave phase shifts calculated for the $V(r)$ potential in the singlet and triplet states (Solid lines). Dotted lines show the curves calculated with $\delta_0 = -a k$.

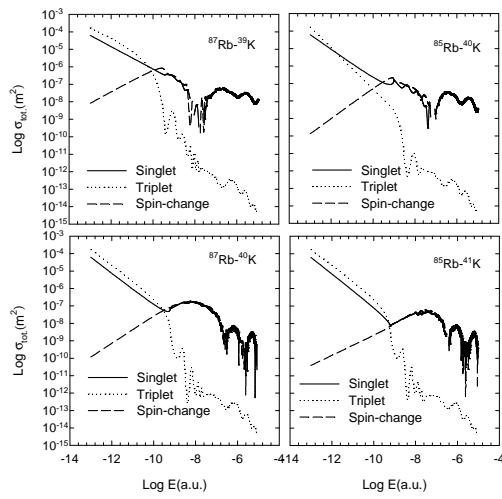


FIG. 4: Cross-sections as a function of the energy in the spin charge, the singlet and triplet states of the mixing of atoms.